33rd Annual International Conference of the IEEE EMBS
Boston, Massachusetts USA, August 30 - September 3, 2011

Rapid Flow Quantification in Iliac Arteries with Spiral Phase-Contrast MRI

MJ Negahdar, Mo Kadbi, Melanie Kotys, Motaz Alshaher,
Stefan Fischer, and Amir A. Amini, IEEE Fellow

Abstract— **Phase contrast MRI is a powerful tool for blood flow quantification. Conventional cartesian phase contrast sequences require lengthy acquisition on the order of several minutes. Spiral acquisition phase-contrast (PC) MRI is capable of reducing the TR and TE in order to minimize flow dependent artifacts and total imaging time. Despite this, in general, spiral phase contrast sequences suffer from off-resonance artifacts and inconsistent data artifacts. In this work, we show that short interleaved spiral readout trajectories have the capability to obtain high spatio-temporal resolution flow images in the common iliac artery distal to the aortoiliac bifurcation with little or no artifacts and with significant savings in image acquisition time over the Cartesian trajectory. To verify the accuracy, we compare our results with a Conventional cartesian trajectory.**

I. Introduction

FLOW visualization and quantification in-vivo is very helpful for diagnosis and monitoring of many vascular and cerebro-spinal diseases. Currently, Doppler ultrasound is a main reference method for vascular and cardiac flow imaging. But existence of air, bone, or surgical scar presents a significant barrier to accurate evaluation [1], [2]. Additionally, Doppler flow imaging can only derive components of velocities in the direction of insonification. As with Ultrasound, magnetic resonance imaging (MRI) has the capability to perform both structural and functional imaging; i.e., it can image the anatomy as well as velocity and flow. Compared to ultrasound however, the direction of velocity encoding can be arbitrarily defined by the operator, and is not limited to being toward or away from the transducer.

Manuscript received April 1, 2011. This work was supported in part by NSF (grant #0730467) and through a grant from the clinical and translational innovative award program at the University of Louisville to Amir Amini

MJ Negahdar is with University of Louisville, Louisville, KY 40292 USA. Phone: 502-852-3400; fax:502-852-1577 (e-mail: m0nega02@louisville.edu).

M. Kadbi is with University of Louisville, Louisville, KY 40292 USA (m0kadb01@louisville.edu).

M. Kotys is with Philips Medical system, Philips Healthcare. Cleveland, OH 44143 USA (melanie.kotys@philips.com).

S. Fischer is with Philips Medical System, Philips Healthcare, Cleveland, OH 44143 USA (stefan.fischer@philips.com).

M. Alshaher is Assistant professor of Medicine (Cardiology) and director of the Cardiac Critical Care Unit at the University of Louisville, Louisville, KY 40202 USA (mmalsh01@louisville.edu)

A. A. Amini is Professor and Endowed Chair in Bioimaging at University of Louisville, Louisville, KY 40292 USA (amir.amini@louisville.edu).

In MR flow imaging, time has a significant role in a method's performance. Low temporal resolution leads to underestimation of peak velocities, and often the total imaging time needs to be limited to the length of a breath-hold. PC MRI is common in blood flow imaging [3] with short imaging times achievable by reducing temporal and spatial resolutions. Fourier Velocity Encoding is more accurate than Phase Contrast MRI in quantification of high speed and complex flows [7], as it is able to extract the spectrum of velocities within each voxel by adding one more frequency dimension related to velocity in the Fourier domain [8]. This idea eliminates partial volume artifact, however, it results in a considerably longer data acquisition time. Quantitative flow measurement methods provide us with a numerical tool to evaluate the amount of flow. Clearly, comparison of measured flow in a diseased vessel with the expected normal flow can be helpful in the diagnosis of patients and can help in understanding and monitoring of the disease process. Quantitative flow measurement methods essentially are based on the accumulated phase of moving spins against stationary ones [9], [11].

II. Phase-contrast MRI

A. Theory

The use of phase contrast to determine fluid velocities was first proposed by Hahn in 1960 [10]. The first application of this method in imaging was developed by Moran [11], and subsequently applied in human cases by Van Dijk [12].

The basis of the phase contrast technique is that spins moving in the presence of a magnetic field gradient acquire a different cumulative phase than stationary spins. For a spatial position vector $r(t)$, and a magnetic field gradient vector $G(t)$, the cumulative phase of the spins in the rotating frame is given by

$$\varphi(t) = \gamma \int_0^t G(\tau).r(\tau)d\tau \qquad (1)$$

where γ is the gyeomagnetic ratio. For simplicity, let us assume that the motion and the gradient are both in the x direction, substituting Taylor's expansion of general equation for a spin's position, x(t), we arrive at

$$\varphi(t) = \gamma x_0 \int_0^t G_x(\tau)d\tau + \gamma v_x \int_0^t G_x(\tau).\tau d\tau + \gamma \frac{1}{2} a_x \int_0^t G_x(\tau).\tau^2 d\tau \quad (2)$$

$$\varphi(t) = \gamma\{x_0 M_0 + v_x M_1 + \frac{1}{2} a_x M_2\} \quad (3)$$

assuming expansion up to the second order. Note that in (3) M_n is the nth moment of the gradient waveform x_0 is initial position v_x is velocity and a_x is acceleration in x direction. Therefore, flow dependent cumulative phase shift depends on initial position, velocity, acceleration, and higher order terms through the gradient's zeroth, first, second, and higher order moments, respectively. If we assume $x_0 = 0$, $a_x = 0$ (constant velocity) and assume higher order terms to be zero, we can rewrite cumulated phase in (3) as follows:

$$\varphi = \gamma v_x M_1 \quad (4)$$

$$v_x = \frac{\varphi}{\gamma M_1} \quad (5)$$

Therefore, by measuring cumulative phase of the spins, it is possible to extract velocity by using (5). Phase values that are greater than π radians cannot be discriminated from their modulus 2π counterparts. So, the velocity corresponding to a phase-shift of π radians defines the upper limit and $-\pi$ the lower limit on the range of velocities that can be accurately measured. It is convenient to define

$$Venc = \frac{\pi}{\gamma \Delta M_1} \quad (6)$$

In that case, the maximum measureable velocity maps to a phase shift of π radians. Any velocity value outside of the range [-Venc +Venc] will be aliased and assigned to a smaller value. The upper limit of the range is referred to as velocity encoding value or Venc [9].

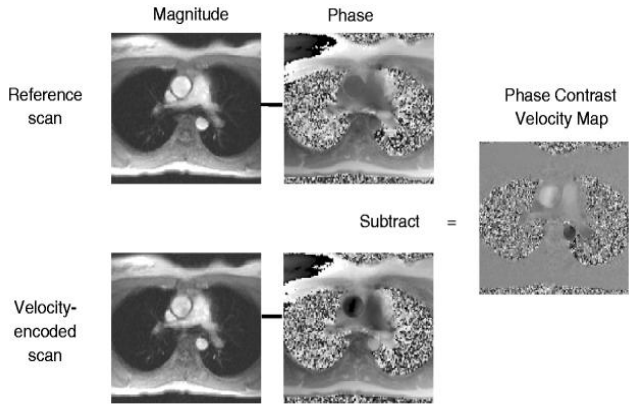

Fig. 1. In PC MRI, the magnitude and phase images are constructed from the reference scan (top row) and also from the velocity encoded scan (bottom row). The corresponding phase images are subtracted resulting in the PC velocity image. Taken from [16].

To remove signal from static tissue and constant noise, often one performs two different acquisitions with identical zero time-moments, and different first time-moment and subsequently subtracts them. Therefore, to construct a velocity image two separate scans are needed. Fig. 1 shows a reference and a velocity encoded scan, and result from phase map subtraction, yielding the velocity map.

The drawback of the PC technique is that the phase can be affected by many undesirable factors like magnetic field in-homogeneity, pulse sequence tuning, acceleration, partial volume artifact, and eddy current [13]-[15]. In addition, PC MR can suffer from data inconsistency and phase dispersion which can degrade the image quality and accuracy [4]-[6].

B. Spin-warp and radial trajectories

Spin-warp uses conventional Cartesian coordinates to cover the k-space (Fig. 2a). Implementation of this method is straightforward; it is sufficient to add a bipolar gradient in desired flow measurement direction of regular imaging sequence. However, this method suffers from off-resonance artifacts due to long echo times. Additionally, relatively long repetition times decrease the temporal resolution in the case of CINE imaging. A motion artifact is another disadvantage of Cartesian scans, causing repetition of moving object in phase-contrast velocity imaging in the phase-encode direction.

Radial phase-contrast has also been developed, but has primarily been used for vessel visualization (for k-space trajectory see Fig. 2b). Barger [17] introduced PIPR (Phase-contrast with Interleaved Projections), an interleaved undersampled projection technique for contrast-enhanced phase-contrast angiography. Relative to Cartesian PC, Radial acquisition can reduce ghosting artifact significantly and it is possible to obtain a higher spatial resolution per unit time. However, because of reduced number of acquisition angles, smearing and streaking artifacts will be visible.

C. Spiral phase contrast

Above considerations provided incentives for having a new strategy for covering the k-space: instead of using horizontal or radial read-out lines in k-space, a spiral read-out trajectory has been proposed for filling the k-space [21]. In this method, the repetition time TR and total scan time can decrease significantly. Unfortunately, the single shot spiral acquisition technique which covers the entire k-space in one read-out leads to severe artifacts. These arise due to off-resonance. In short, since the entire k-space is scanned in one shot, while the MR signal is undergoing T2 decay and signal dephasing, the SNR is reduced in time and by the time the high-frequency portions of k-space is reached very little signal is left. Finally in single-shot imaging in our case, each read-out and each velocity image will take in the range of 124-128 ms and 258-266 ms respectively, therefore, Cine

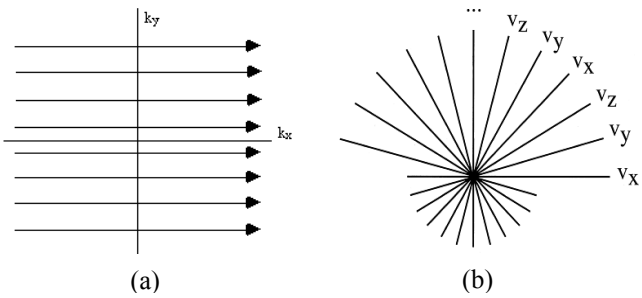

Fig. 2. K-space trajectory for (a) Cartesian and (b) radial acquisitions. Taken from [http://users.fmrib.ox.ac.uk/~stuart/thesis/] and [17].

imaging is not possible due to the long read-out times and poor temporal resolutions (e.g., 2-3 images per cardiac cyle). Pike [18] suggested an interleaved spiral k-space acquisition. The advantage of this method is its capability to significantly reduce TR, removing respiratory ghosting, among others. Moreover, since in the interleaved approach the center of the k-space is sampled multiple times, resulting in higher data density at the origin, pulsatile-flow related artifacts are reduced [19].

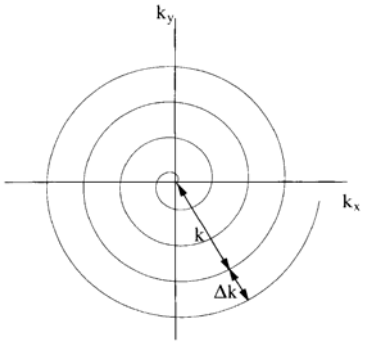

Fig. 3. K-space trajectory of a uniform density single shot spiral showing sample spacing Δk, in the radial direction. Taken from [20]

Fig. 3 shows the k-space trajectory of a uniform density single shot spiral. The shape of the gradient waveforms in spiral MRI is different from the gradient waveform in Cartesian and radial MRI; equations (7-9) show the expressions for the spiral gradient waveforms:

$$k_x = k(t)\cos(\theta(t)) \tag{7}$$

$$k_y = k(t)\sin(\theta(t)) \tag{8}$$

$$k(t) = A \cdot \theta(t) \tag{9}$$

Where A is a constant, and is determined by the Nyquist criterion. If Δk is radial distance advanced by one rotation, D is the size of FOV, and M the number of interleaves, to satisfy the Nyquist criterion for uniform density spiral trajectories.

$$\Delta k \le \frac{M}{D} \tag{10}$$

In interleaved spiral phase contrast instead of using one long spiral arm with N rotations, N short spiral interleaves with one rotation can be used (fig. 4). With this approach, the total read-out time required to cover entire of k-space stays the same but density of data sampling increases at the origin leading to higher accuracy and SNR in reconstruction. Fig. 4 demonstrates conventional single shot spiral and interleaved spiral trajectories for covering identical regions in k-space.

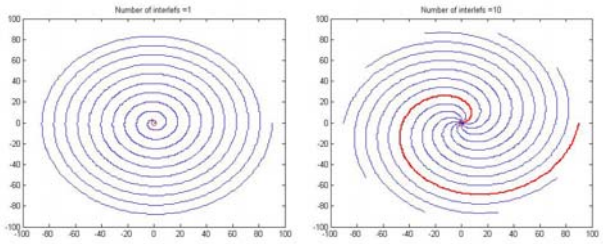

Fig. 4. Demonstartion of (a) conventional single shot spiral acquisition with 10 rotations and (b) interleved spiral acquisition with 10 interleaves.

Although the Nyquist rate is satisfied in both cases, with interleaved spiral, a higher data density is achieved at the origin of k-space. Additionally, with interleaved acquisitions (with M interleaves), the total read-out time is separated into M shorter read-out times, resulting in less dephasing in outer part of k-space and off-resonance artifacts.

III. Materials and Methods

Imaging was performed on a Philips Achieva 3T scanner (Philips Healthcare, Best, NL). The flow waveforms were calculated in a normal 29 year old male volunteer. To measure flow, we used a turbo gradient echo sequence (turbo factor = 3), which included a bipolar flow encoding gradient with a short spiral readout. To take full advantage of the fast acquisition of a spiral read-out and to concurrently avoid off-resonance artifacts, as discussed in section II, we used several sparse and short spiral interleaves, thus reducing flow artifacts associated with a large read-out 1st moment. To assess the impact of the number of spiral interleaves on accuracy of velocities in the iliac arteries, different numbers of interleaves were tested (Table I). The sequence parameters were also optimized to minimize artifacts while maintaining a high SNR.

Fig. 5 demonstrates our designed spiral phase contrast pulse sequence for imaging velocities in the iliac arteries. It consists of (a) short and selective RF pulse to minimize echo time and in-plane flow artifacts, (b) bipolar flow encoding gradient in direction of flow, (c) short spiral read-out gradients to mitigate off resonance artifact, and (d) refocusing and spoiler gradients to eliminate residual transverse magnetization. The TR/TE = 7.0/2.6 ms were optimized to maximize temporal resolution and reduce flow artifacts, respectively. Each velocity image takes 2*TR = 14 ms to acquire; consequently, about 63 phase images can be acquired in one heart beat (assuming useable time in the R-R

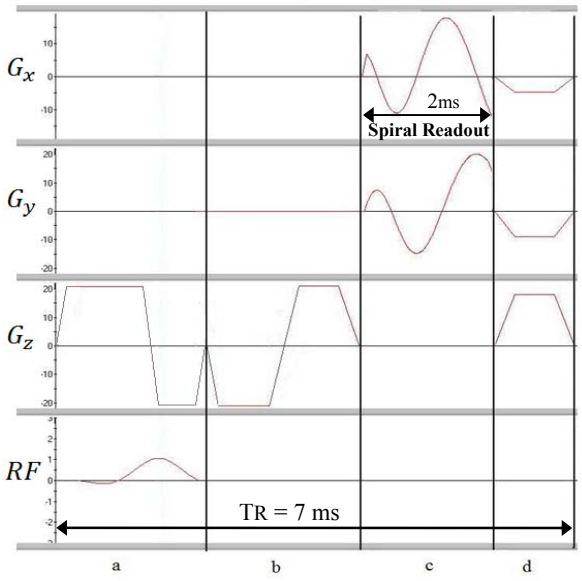

Fig. 5. Interleaved Spiral Phase Contrast pulse sequence. It consists of (a) slice selective excitation pulse, (b) velocity encoding bipolar gradient, (c) short spiral readout, and (d) refocusing and spoiler gradients.

interval to be about 900 ms). Using a turbo factor of 3 in turbo gradient echo sequence reduces the number of phase images to 21. Short echo time was achieved by using a 10º flip angle and a short RF excitation pulse (750 µs).

The remaining sequence parameters were as follows: FOV = 250x250 mm, 1.5 x 1.5 mm acquired in-plane resolution, 5 mm slice thickness, and 168 x 168 matrix size. In order to minimize the off-resonance artifacts, the read-out time was decreased to 2 ms. To provide sufficient k-space coverage, the number of spiral interleaves was increased to 75. With a turbo factor of 3, 25 heart beats are required to acquire all 75 interleaves. To avoid velocity aliasing, a Venc of 100 cm/sec was used for imaging both iliac arteries.

The turbo gradient echo PC sequence with Cartesian readout was also implemented with the minimum possible TE = 4.1 ms, but otherwise had the same parameters as specified above for the Spiral sequence.

The Cartesian phase contrast scans were used as reference scan in order to measure the accuracy of the proposed spiral phase contrast technique. To determine accuracy, the flow waveform obtained both the spiral and the Cartesian scans were compared using the root mean-squared error (RMSE) criterion.

$$RMSE = \sqrt{\frac{1}{n}\sum (Q_S - Q_C)^2} \qquad (11)$$

where n is the number of phases, Q_c is the flow waveform as quantified with the Cartesian sequence, and Q_s is the flow waveform as quantified with the Spiral sequence.

IV. RESULTS

Fig. 6 demonstrates the flow waveforms in a normal subject at identical slice locations. Both curves have the same shape and peak flow. However, the total imaging time was significantly reduced from 56 heart-beats with a Cartesian readout to 25 heart-beats with the spiral readout. Fig. 7 demonstrates flow waveforms as in fig. 6 but with the number of spiral interleaves reduced from 75 to 30. In fact, table I illustrates that decreasing the number of interleaves from 75 to 30 leads to shorter total imaging time (26 heart beats to 11 heart beats) with a small loss of accuracy in the quantified flow waveform based on the RMSE criterion.

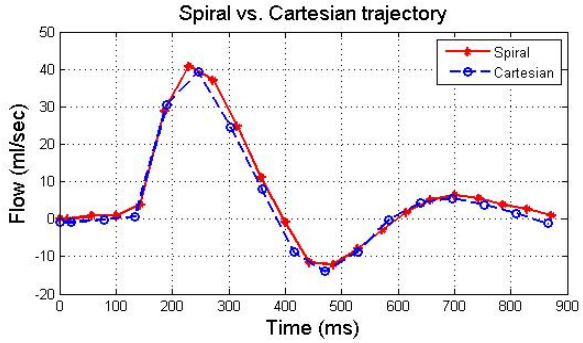

Fig. 6. Flow waveform in left Iliac artery for spiral and Cartesian acquisition over the cardiac cycle for 75 spiral interleaves.

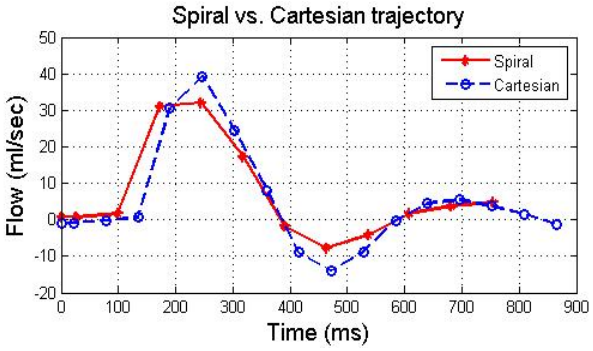

Fig. 7. Flow waveform in left Iliac artery for spiral and Cartesian acquisition over the cardiac cycle for 30 spiral interleaves. Although with much less interleaves, the shape of flow waveform was maintained

A further advantage of the spiral acquisition which was observed was the reduction of motion artifacts commonly seen in flow imaging with the Cartesian trajectory (Fig. 8).

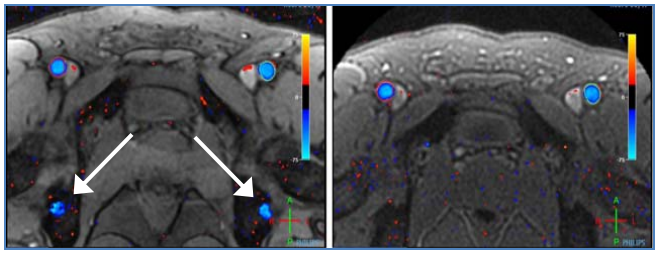

(a) (b)

Fig. 8. Color overlay of phase on magnitude image in the iliac arteries. (a) White arrows show the flow-induced ghosting artifacts visible in Cartesian scan. (b) This is resolved with the spiral read-out. Both images are in the same person and at the same axial location.

Table I. Comparison of spiral and cartesian acquisition for different number of spiral interleaves

Readout	# of interleaves	TR/TE (msec)	read-out time (msec)	Max # of phases	Total imaging time (seconds)	RMSE (mm^3 /sec)
Cartesian (Reference)	-----	7.0/4.1	3.6	21	56	0
Spiral	75	7.0/2.6	2	21	26	1.99
Spiral	51	7.8/2.6	2.8	19	18	3.15
Spiral	30	9.3/2.6	4.3	16	11	5.23

V. Discussion and conclusions

In this work we designed an optimized spiral phase contrast sequence to acquire high temporal resolution velocity images in the iliac arteries. Using a small voxel size (1.5x1.5x5 mm) reduced the partial volume artifact and improved the accuracy of phase images.

Motion artifacts observed in Cartesian acquisitions were not visible in results obtained with the proposed spiral acquisition while the total imaging time decreased significantly without affecting accuracy of velocity image. It was also observed that although reducing the number of spiral interleaves degrades the quality of the magnitude image, the quality of the phase image was to a large degree maintained. Also obtaining short repetition time (TR=7ms) provides high temporal resolution and the capability for fast flow imaging. Moreover short read-out time reduced the effect of off resonance due to long read-out time in conventional single shot spiral acquisition.

Although there are some advantages to use of spiral acquisitions, there are also challenges. The common disadvantage of non-Cartesian trajectories comes from the basic definition of the Discrete Fourier Transform which requires Cartesian gridded data as input. This requirement forces us to regrid non-Cartesian data into a Cartesian grid prior to applying inverse Fourier transformation, resulting in interpolation errors. On the other hand we need to apodize the image by multiplying with the inverse Fourier transform of the interpolation kernel. Also in the case of 3D velocity measurement, when using the Cartesian trajectory, we can use the same reference scan for all three velocity encoded directions. This improves the temporal resolution from 6TR to 4TR. However, this is not possible with spiral acquisitions. Finally, use of single shot spiral readout leads to off resonance in outer parts of k-space due to spins dephasing.

We believe due to sparsity of MR images and coherence between successive phase images in cine phase contrast imaging, combining partial Fourier sampling and parallel imaging with spiral acquisition can further reduce imaging time while resulting in less data inconsistency and off-resonance artifacts. This line of research is already being pursued by researchers [22] including in cardiac imaging [23] and should prove useful in vascular imaging.

References

[1] A. J. Winkler and J. Wu, "Correction of intrinsic spectral broadening errors in doppler peak velocity measurements made with phased sector and linear array transducers," Ultrasound in Medicine & Biology, vol. 21, pp. 1029-1035, 1995.

[2] P. R. Hoskins, "Accuracy of maximum velocity estimates made using Doppler ultrasound systems," Br J Radiol, vol. 69, pp. 172-177, February 1, 1996.

[3] M. O'Donnell, "NMR blood flow imaging using multiecho, phase contrast sequences," Med Phys, vol. 12, pp. 59-64, Jan-Feb 1985.

[4] G. D. Clarke, W. G. Hundley, R. W. McColl, R. Eckels, D. S. C. Chaney, et al., "Velocity-encoded, phase-difference cine MRI measurements of coronary artery flow: Dependence of flow accuracy on the number of cine frames," Journal of Magnetic Resonance Imaging, vol. 6, pp. 733-742, 1996.

[5] C. Tang, D. D. Blatter, and D. L. Parker, "Accuracy of phase-contrast flow measurements in the presence of partial-volume effects," Journal of Magnetic Resonance Imaging, vol. 3, pp. 377-385, 1993.

[6] K. S. Nayak, B. S. Hu, and D. G. Nishimura, "Rapid quantitation of high-speed flow jets," Magn Res in Med, vol. 50, pp. 366-372, 2003.

[7] J. L. A. Carvalho, J.-F. Nielsen, and K. S. Nayak, "Feasibility of in vivo measurement of carotid wall shear rate using spiral fourier velocity encoded MRI," Magn Res in Med, vol. 63, pp. 1537-1547, 2010.

[8] D. G. Nishimura, Principles of Magnetic Resonance Imaging: Stanford Univ, 2010.

[9] N. J. Pelc, F. G. Sommer, K. C. Li, T. J. Brosnan, R. J. Herfkens, and D. R. Enzmann, "Quantitative magnetic resonance flow imaging," Magn Reson Q, vol. 10, pp. 125-47, Sep 1994.

[10] E. L. Hahn, "Detection of Sea-Water motion by nuclear precession," Journal of Geophysical Research, vol. 65, pp. 776-777, 1960.

[11] P. R. Moran, "A flow velocity zeugmatographic interlace for NMR imaging in humans," Magnetic Resonance Imaging, vol. 1, pp. 197-203, 1982.

[12] P. Van Dijk, "Direct cardiac NMR imaging of heart wall and blood flow velocity," Journal of Computer Assisted Tomography, vol. 8, pp. 429-436, 1984.

[13] M.Markl,"Velocity encoding and flow Imaging," Available: http://mrel.usc.edu/ class/591/library/MarklFlowImaging.pdf, 2005

[14] M. A. Gonzalez Ballester, A. P. Zisserman, and M. Brady, "Estimation of the partial volume effect in MRI," Medical Image Analysis, vol. 6, pp. 389-405, 2002

[15] T. Miller, A. Landes, and A. Moran, "Improved accuracy in flow mapping of congenital heart disease using stationary phantom technique," J. of Cardiovasc. Magn Reson, vol. 11, p. 52, 2009.

[16] P. Gatehouse, J. Keegan, L. Crowe, S. Masood, R. Mohiaddin, et al., "Applications of phase-contrast flow and velocity imaging in cardiovascular MRI," Euro Radiology, vol. 15, pp. 2172-2184, 2005.

[17] A. V. Barger, D. C. Peters, W. F. Block, K. K. Vigen, F. R. Korosec, et al., "Phase-contrast with interleaved undersampled projections," Magnetic Resonance in Medicine, vol. 43, pp. 503-509, 2000.

[18] G. B. Pike, C. H. Meyer, T. J. Brosnan, and N. J. Pelc, "Magnetic resonance velocity imaging using a fast spiral phase contrast sequence," Magnetic Resonance in Medicine, vol. 32, pp. 476-483, 1994.

[19] D. G. Nishimura, P. Irarrazabal, and C. H. Meyer, "A velocity k-space analysis of flow effects in echo-planar and spiral imaging," Magn Reson Med, vol. 33, pp. 549-56, Apr 1995.

[20] K. F. King, T. K. Foo, and C. R. Crawford, "Optimized gradient waveforms for spiral scanning," Magn Reson Med, vol. 34, pp. 156-60, Aug 1995.

[21] C. B. Ahn, J. H. Kim, and Z. H. Cho, "High-Speed Spiral-Scan Echo Planar NMR Imaging-I," Medical Imaging, IEEE Transactions on, vol. 5, pp. 2-7, 1986.

[22] M. Lustig and J. M. Pauly, "SPIRiT: Iterative self-consistent parallel imaging reconstruction from arbitrary k-space," Magnetic Resonance in Medicine, vol. 64, pp. 457-471, 2010.

[23] N. Seiberlich, G. Lee, P. Ehses, J. Duerk, and M. Griswold, "Through-time spiral GRAPPA for real-time cardiac imaging," Proc. of ISMRM, abstract # 4392, Montreal, Canada, May 2011.